

7.5 MEAN, TIDAL, AND FLUCTUATING WINDS IN THE MIDDLE ATMOSPHERE AND  
LOWER THERMOSPHERE OBSERVED DURING MAP/WINE  
IN NORTHERN SCANDINAVIA

J. Röttger

EISCAT Scientific Association  
P. O. Box 812  
S-981 28 Kiruna, Sweden

During the MAP/WINE campaign in winter 1983/84 several instrumental techniques, such as meteorological rockets, sounding rockets, MST radar and incoherent scatter radar, were applied to measure wind velocities in the middle atmosphere. Profiles of mean, tidal and fluctuating wind velocities were obtained up to 90 - 100 km altitude. These are compared with profiles from models, measurements at other locations and at other times as well as satellite-derived data. The results are discussed in terms of ageostrophic winds, planetary waves, tidal modes and the possibility of a saturated gravity wave spectrum in the mesosphere.

Observations of mean, tidal and fluctuating winds in the lower thermosphere and middle atmosphere during MAP/WINE

deduced from measurements with

Rockets:  
data sondes  
chaff clouds  
falling spheres

MST Radar

Incoherent Scatter Radar

Publications

- W. Meyer: Untersuchungen groß und kleinskaliger dynamischer Prozesse in der Mesosphäre anhand von Wind- und Dichtemessungen über Nordskandinavien im Rahmen des MAP/WINE Projekts, Bonn University, 1988.
- W. Meyer, C. R. Philbrick, J. Röttger, R. Rüster, H.-U. Widdle, and F. J. Schmidlin, Mean winds in the winter middle atmosphere above northern Scandinavia, *J. Atmos. Terr. Phys.*, **49**, 675, 1987.
- J. Röttger, and W. Meyer, Tidal wind observations with incoherent scatter radar and meteorological rockets during MAP/WINE, *J. Atmos. Terr. Phys.*, **49**, 689, 1987.
- H. Hass, and W. Meyer, Gravity wave fields above Andöya, *J. Atmos. Terr. Phys.*, **49**, 705, 1987.
- H.-U. Widdel, Vertical movements in the middle atmosphere derived from foil cloud experiments, *J. Atmos. Terr. Phys.*, **49**, 723, 1987.
- R. Rüster, and J. Klostermeyer, Propagation of turbulence structures detected by VHF radar, *J. Atmos. Terr. Phys.*, **49**, 743, 1987.
- E. V. Thrane, T. A. Blix, C. Hall, T. L. Hansen, U. von Zahn, W. Meyer, P. Czechowsky, G. Schmidt, H. -U. Widdel, and A. Neumann, Small scale structure and turbulence in the mesosphere and lower thermosphere at high latitudes in winter, *J. Atmos. Terr. Phys.*, **49**, 751, 1987.

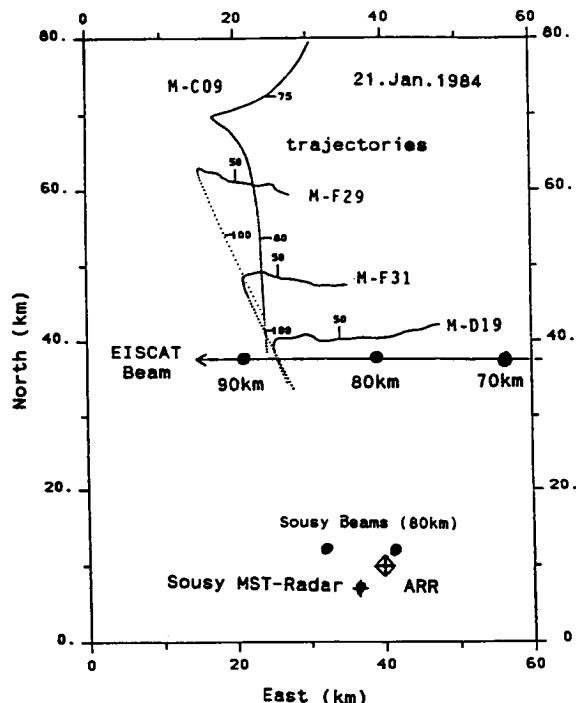


Figure 1. MAP/WINE radar and rocket geometry [after Meyer, 1988].

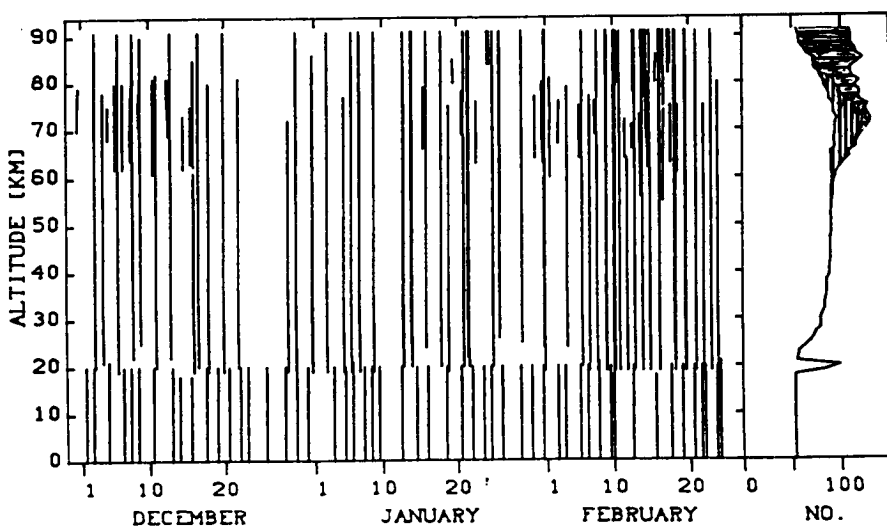


Figure 2. Distribution in time of wind profiles obtained during the period of rocket launched at Andöya ( $69^{\circ}\text{N}$ ,  $16^{\circ}\text{E}$ ). Total number of measurements used for mean wind reduction (right panel); rocket measurements (blank), MST radar (vertically dashed), EISCAT (horizontally dashed). W. Meyer et al.

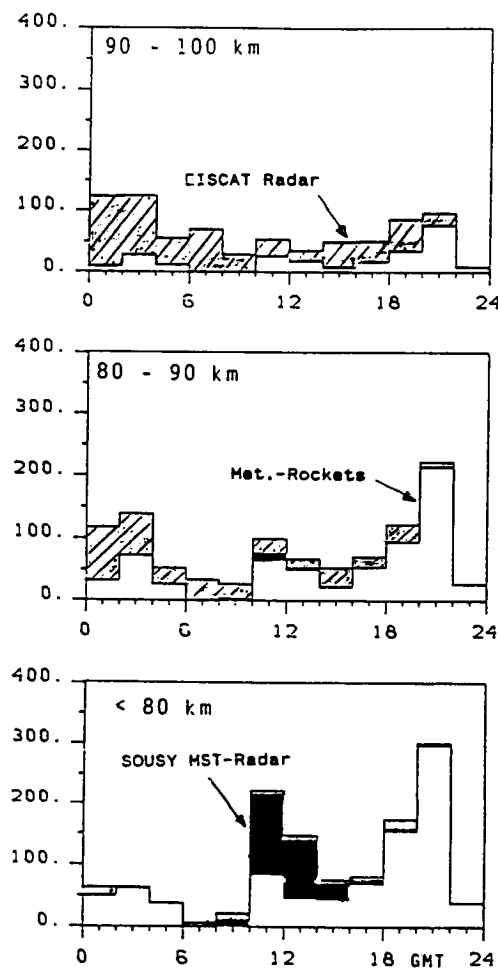


Figure 3. Daily distribution of wind measurements. Meyer [1988].

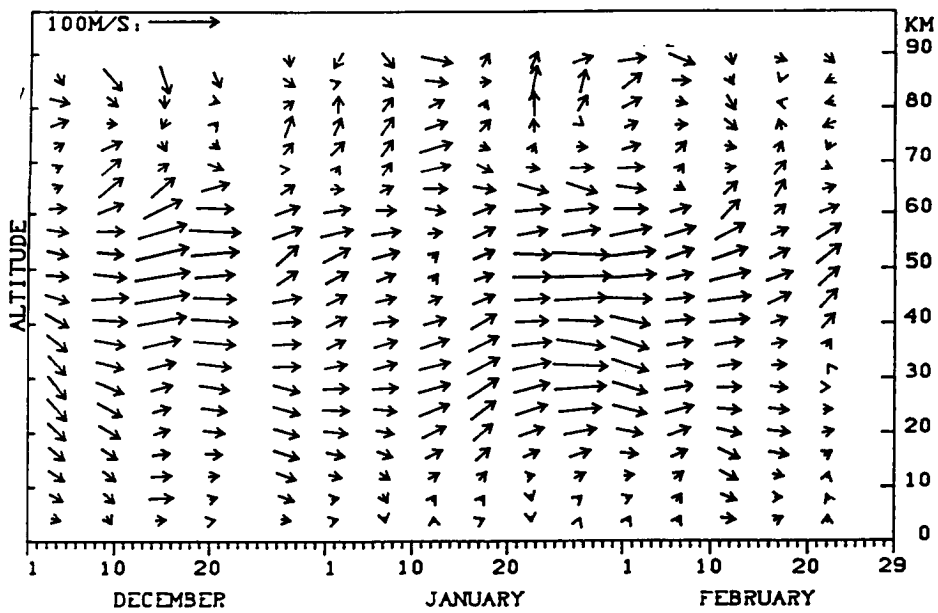
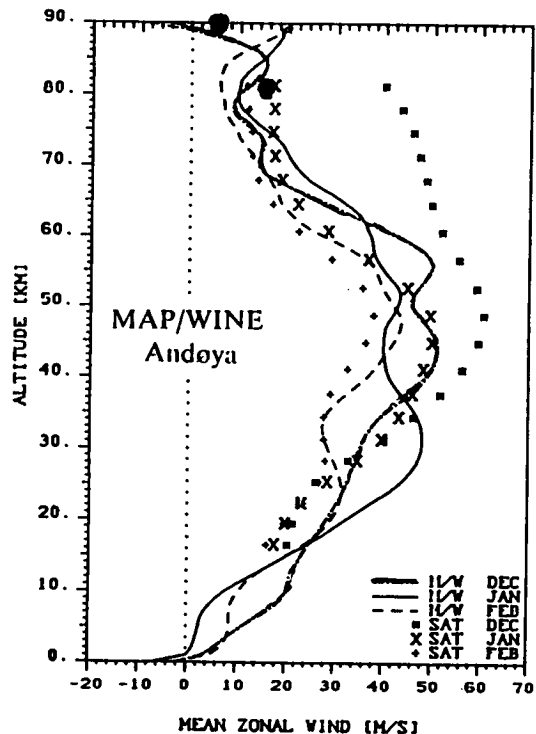


Figure 4. The estimated prevailing wind field above Andöya. Arrows indicate magnitude and direction of the horizontal flow (from the south: upward, from the west: to the right). W. Meyer et al.

W. MEYER *et al.*

D. B. BALSLEY AND A. C. RIDDLE

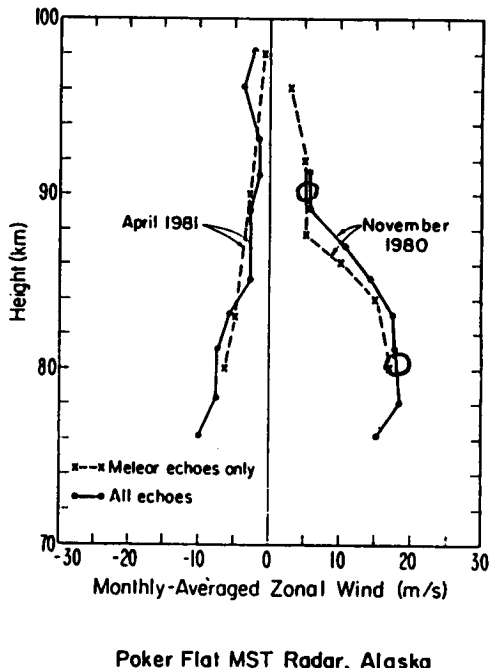


Figure 5. Mean wind profiles during MAP/WINE and at Poker Flat. Meteorological rockets, sounding rockets and radar systems satellite derived winds.

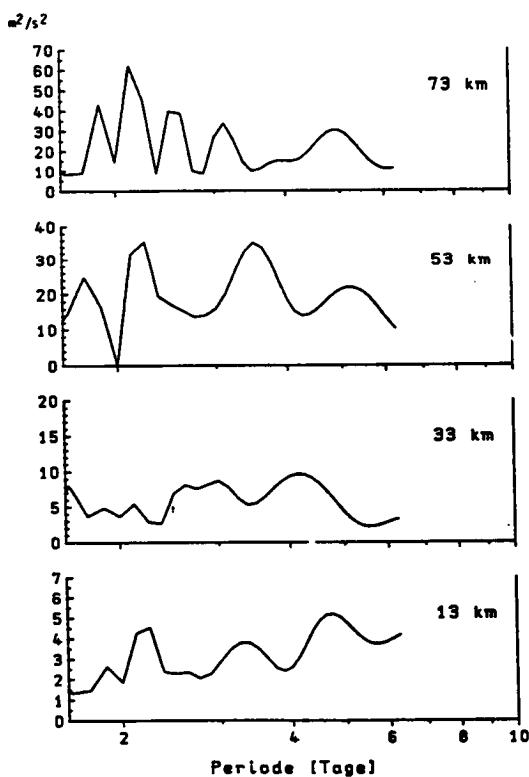


Figure 6. Spectrum of meridional wind component. Meyer [1988].

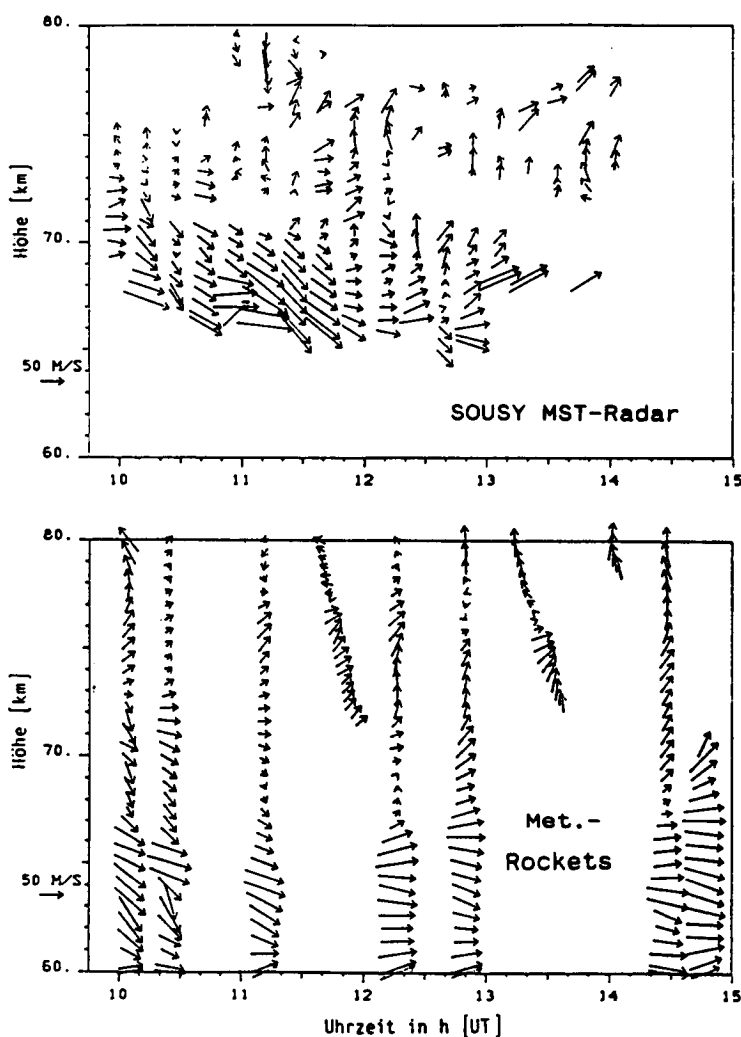


Figure 7. Horizontal wind vectors on 21 January 1984. Horizontale Windvektoren (Südwind: nach oben, Westwind: nach rechts) am 21 Januar gemessen mit dem SOUSY-MST radar (oben) und meteorologischen Raketen (unten). Meyer [1988].

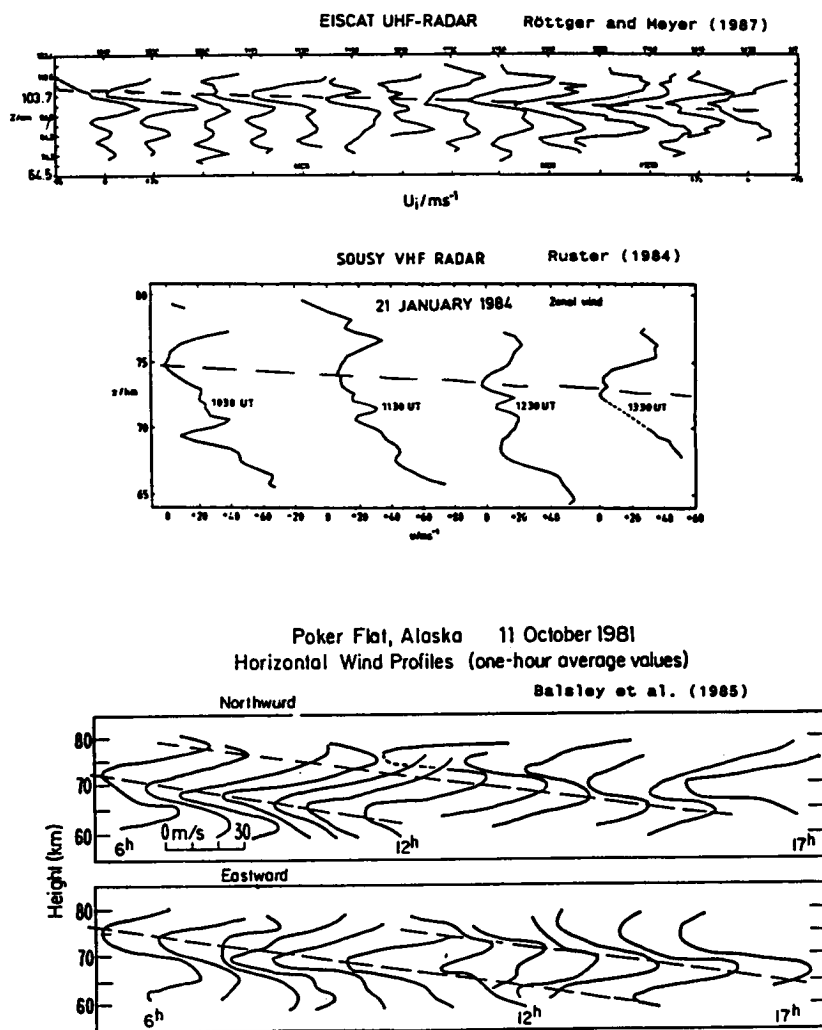
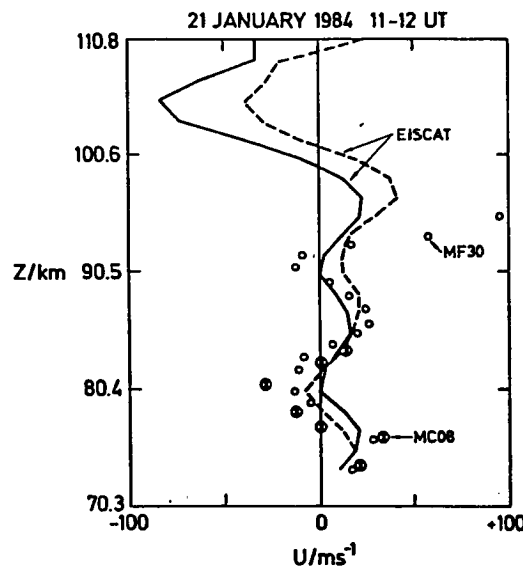
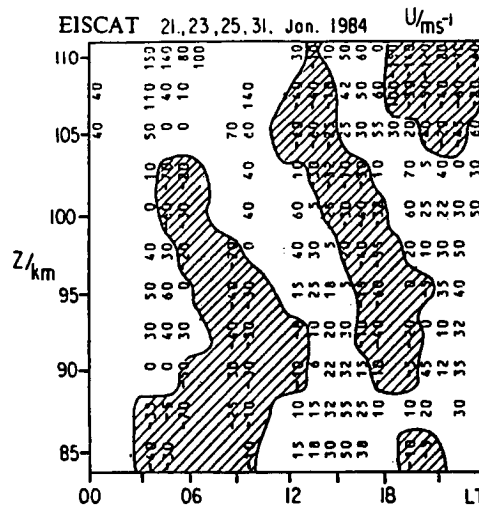


Figure 8. Horizontal wind vectors on 21 January 1984. Meyer [1988].



**Figure 9.** Zonal velocity profiles measured with EISCAT using the matched filter velocity estimates (solid curve 1111 - 1120 UT, dashed curve 1131 - 1140 UT) and falling sphere MF30 (1107 UT) and chaff MC08 (1131 UT) during metrocket salvo 1 on 21 January 1984. Röttger and Meyer [1987].



**Figure 10.** From J. Röttger and W. Meyer.

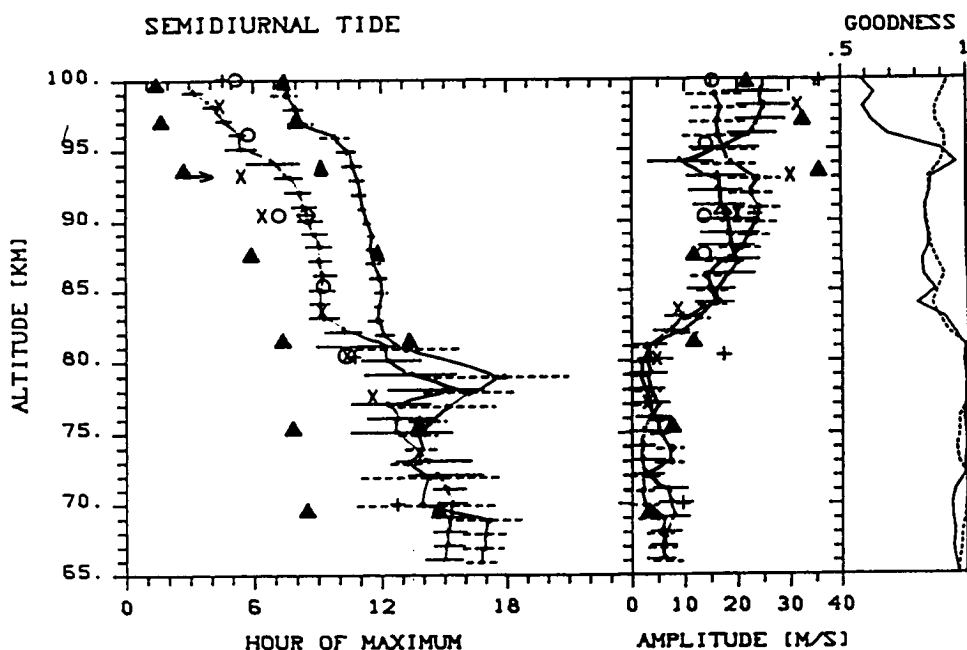


Figure 11. Profiles of amplitude and phase (hour of maximum velocity) of zonal (dashed bars) and meridional (continuous bars) semidiurnal velocity components deduced from all incoherent scatter radar, meteorological rocket and MST radar data. The special characters indicate the maximum of the meridional tidal component (if only zonal components were available, they were shifted by 3 h) obtained from: ▲ Forbes model at 70°N during December solstice [Forbes and Gillette, 1982]; X winter average of Garchy (48°N) [Fellous et al., 1975]; + average over two winters in Saskatoon [Manson et al., 1983]; ◆ vector average over four winters in Saskatoon [Manson et al., 1983]; O 5-day global average deduced from ATMAP high latitude data ( $> 43^\circ$ ) of December 1983 [Forbes, 1985]. J. Röttger and W. Meyer.

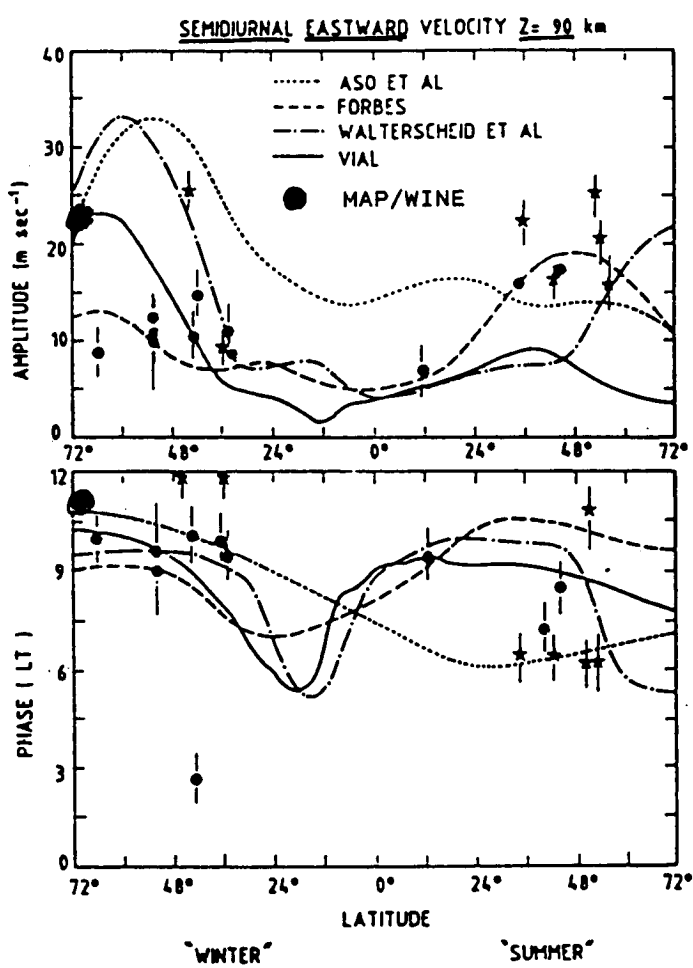


Figure 12. From Forbes [1985].

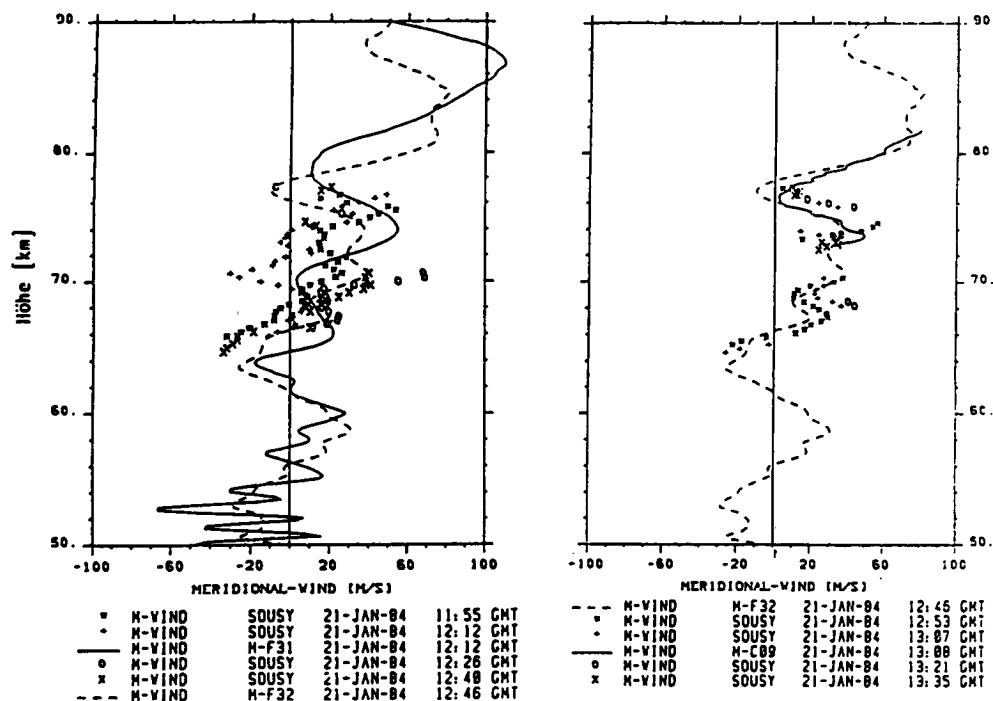


Figure 13. Meridional wind measured with MST radar and rockets. Meyer [1988].

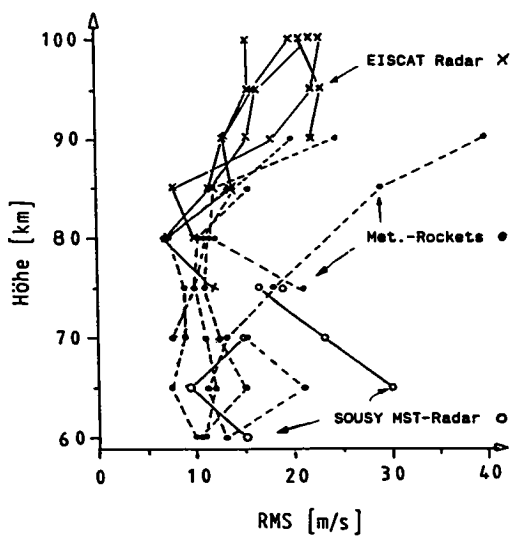


Figure 14. Horizontal wind variations (6 h-rms) Meyer [1988].

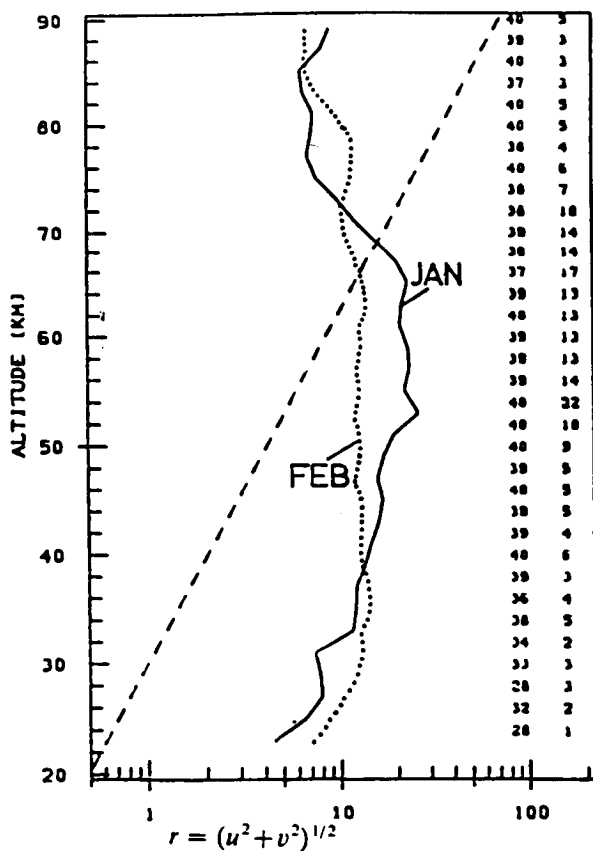
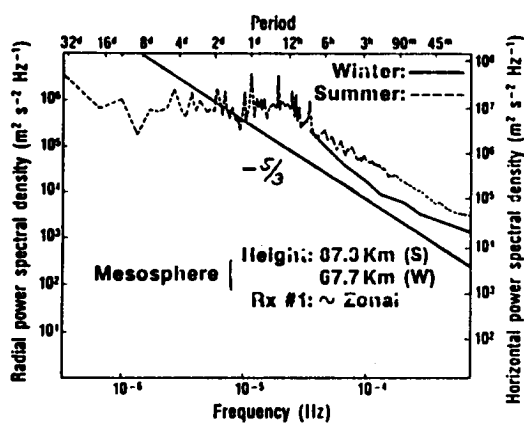


Figure 15. Height profiles of mean horizontal wind fluctuations. H. Hass and W. Meyer.

**Poker Flat, Alaska**  
**Horizontal Power Spectral Densities**

Daisley and Garcillo



**MOBILE SOUSY RADAR**

P. Czechowsky and R. Ruster

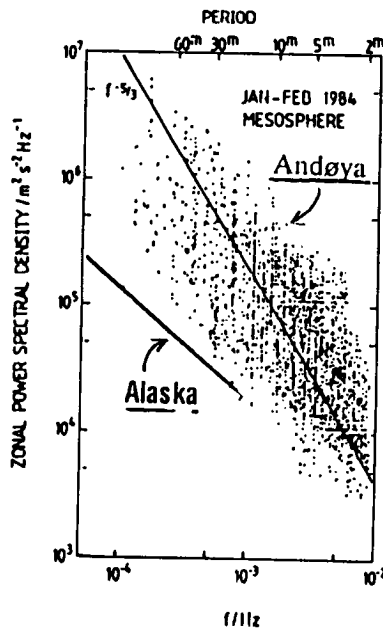
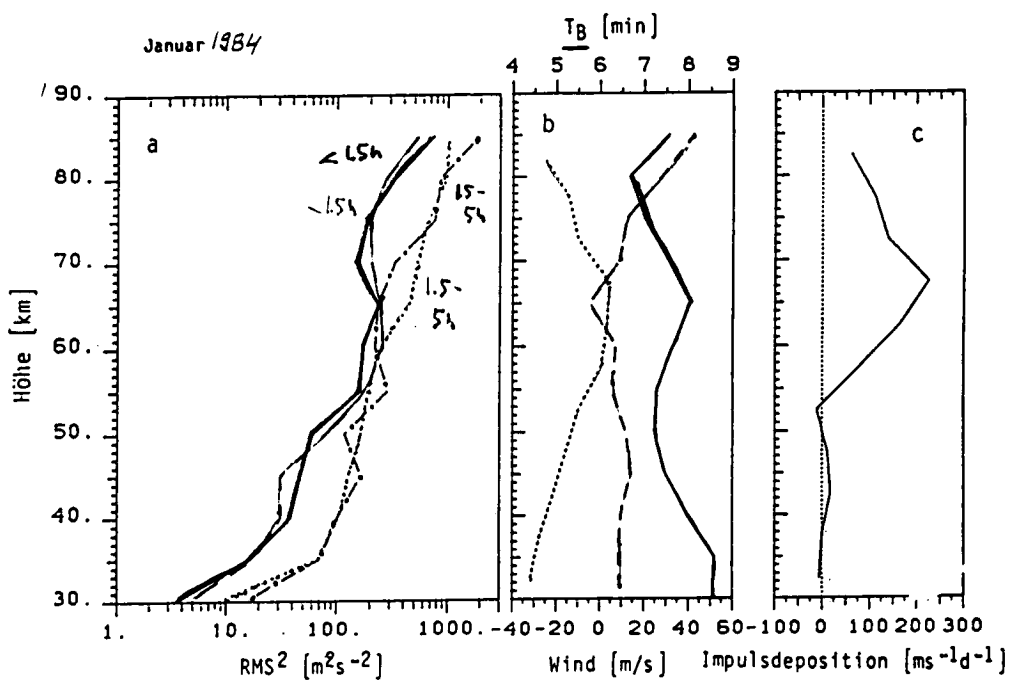


Figure 16.



**Figure 17.** Velocity variability, mean wind and horizontal acceleration. (a) (links): Kurzzeitvariabilität der zonalen (durchgezogen) und meridionalen (strichliert) Windkomponente für Zeitdifferenzen < 1,5 h und 1,5 - 5 h (zonal: strich-punktiert, meridional: punktiert) unter Verwendung von Messungen mit meteorologischen Raketen. (b) (mitte): mittlerer zonaler (durchgezogen) und meridionaler (strichliert) Wind und Brunt-Väisälä-Periode (punktiert). (c) (rechts): Abschätzung der Impulsdeposition aus (a). Meyer [1988].

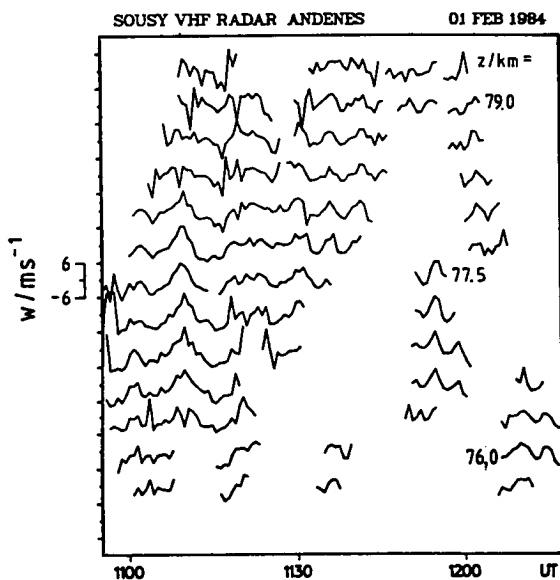


Figure 18. Time variation of vertical velocity  $w$  at heights between 76 and 79 km. R. Rüster and J. Klostermeyer.

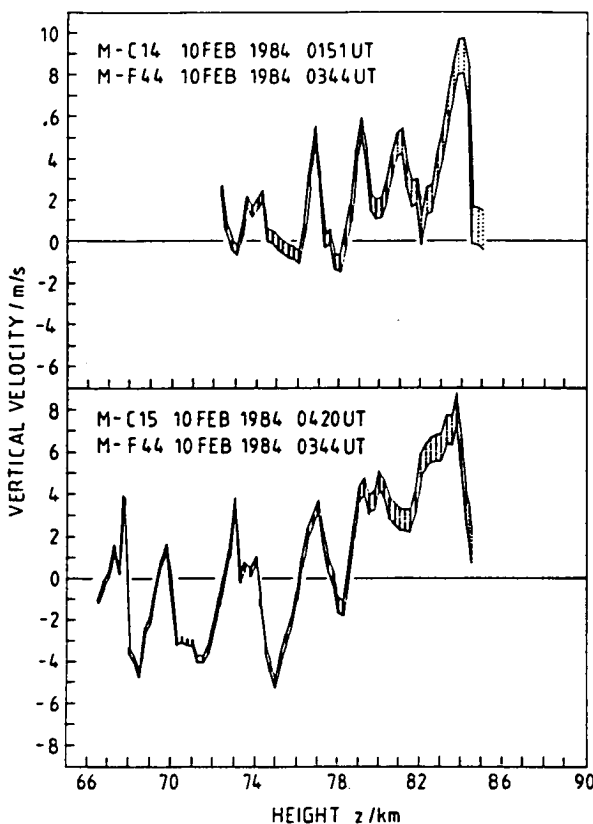


Figure 19. Vertical velocities determined by foil clouds during the fourth salvo (10 February 1984). On both occasions the chaff cloud was intercepted by a wave with upgoing phase which drifted with the wind. H.-U. Widdel.

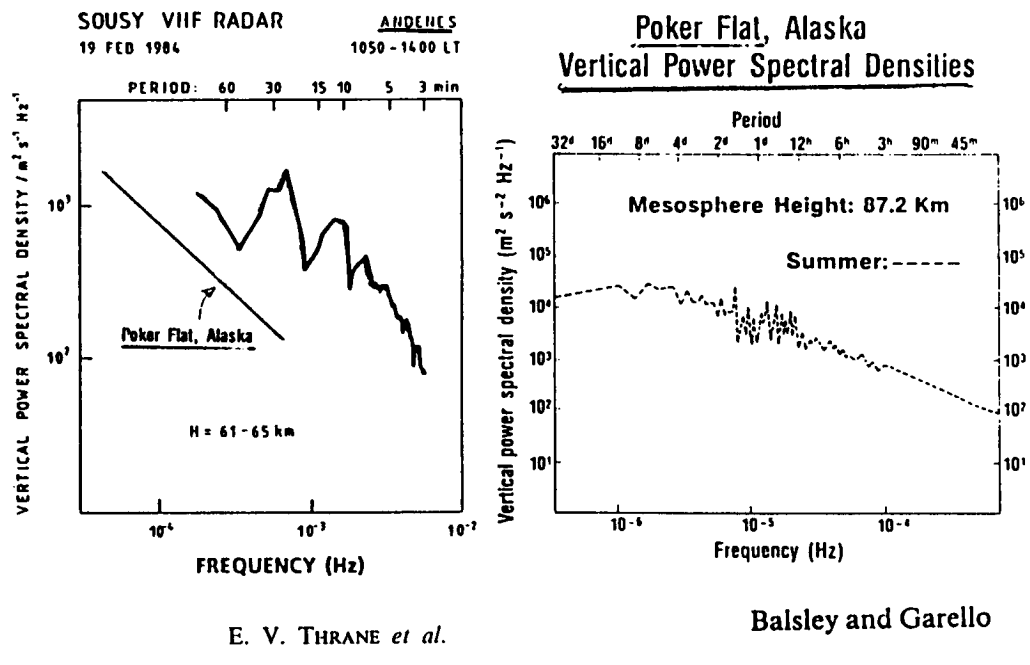


Figure 20.

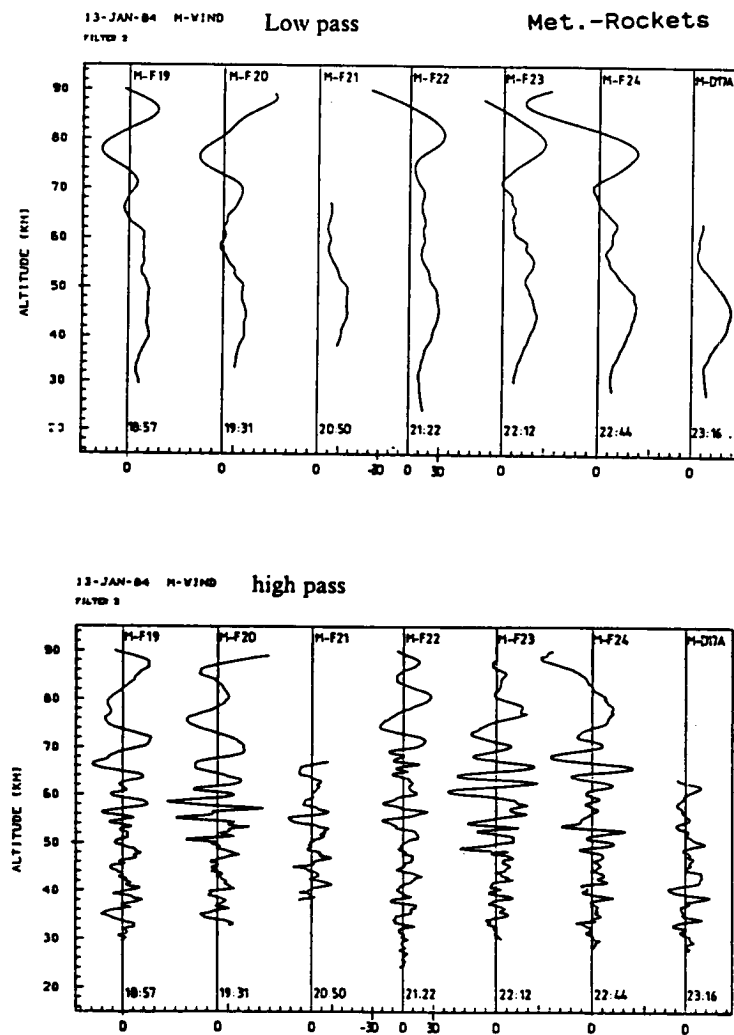


Figure 21. Meridional wind profiles. H. Hass and W. Meyer.

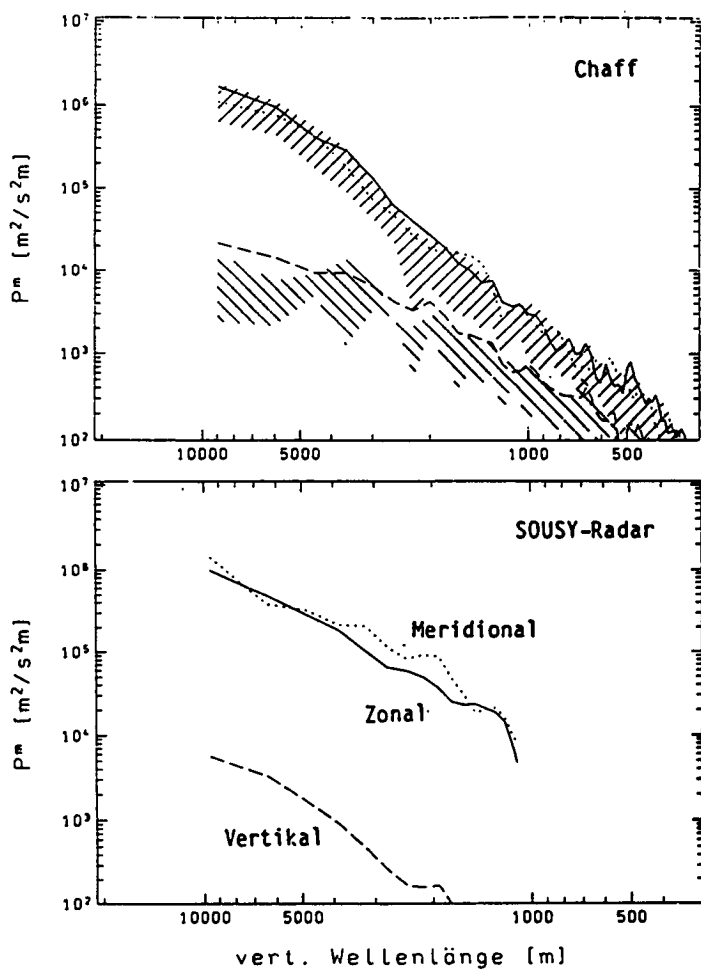


Figure 22. Vertical wave number spectrum. Meyer [1988].

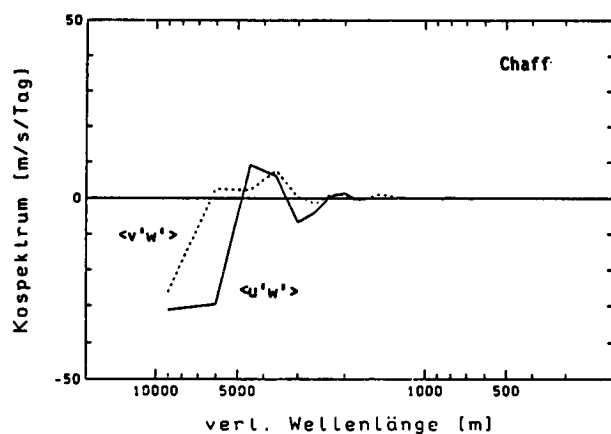
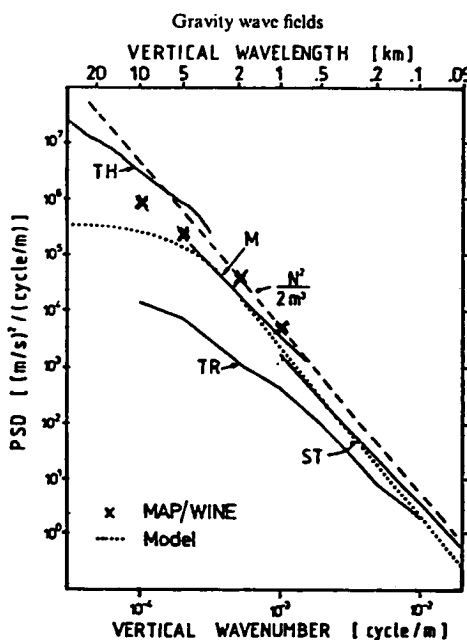


Figure 23. Covariances as function of vertical wave number. Meyer [1988].



**Figure 24.** Comparison of observed spectral densities with model spectra [adopted from Smith et al., 1986]. TH = thermospheric spectrum; M = mesospheric spectrum [both Smith et al., 1986]; ST = stratospheric spectrum [Dewan et al., 1984]; TR = tropospheric spectrum [Endlich et al., 1969]; crosses are average of M-F and M-D spectra. Model spectra: dashed line according to equation (i) with  $N = 0.02 \text{ rad s}^{-1}$  and dotted line with equation (9) and  $m_*^{-1} = 5 \text{ km}$ . H. Hass and W. Meyer.

#### Summary of Middle Atmosphere Dynamics (excl. turbulence) over Northern Scandinavia during Winter 1983/1984 (MAP/WINE)

##### \*Prevailing Winds:

Zonal component is geostrophic, meridional component is ageostrophic in mesosphere.

\*Indications of Planetary Waves ( $T \sim 2d$ ?).

\*Semidiurnal tide is dominant above mesopause.

\*Short-period gravity waves ( $T < 6\text{h}$ ) appear to saturate above the lower mesosphere; northern Europe (MAP/WINE) more "active" than Alaska?

\*Indication of momentum deposition by short-period gravity waves.